

## Multifractal eigenstates of quantum chaos and the Thue-Morse sequence

N. Meenakshisundaram and Arul Lakshminarayan

Department of Physics, Indian Institute of Technology Madras, Chennai, 600036, India

(Received 17 December 2004; published 28 June 2005)

We analyze certain eigenstates of the quantum baker's map and demonstrate, using the Walsh-Hadamard transform, the emergence of the ubiquitous Thue-Morse sequence, a simple sequence that is at the border between quasiperiodicity and chaos, and hence is a good paradigm for quantum chaotic states. We show a family of states that are also simply related to the Thue-Morse sequence and are strongly scarred by short periodic orbits and their homoclinic excursions. We give approximate expressions for these states and provide evidence that these and other generic states are multifractal.

DOI: 10.1103/PhysRevE.71.065303

PACS number(s): 05.45.Mt, 03.65.Sq

The emergence of nonlinearity-induced chaos from the linear Schrödinger equation in the classical limit is a subtle and interesting phenomenon [1–3]. The eigenstates of quantized chaotic systems are of current interest. They range from those that bear striking resemblance to classical periodic orbits, and hence are called “scarred states” [2], to those that are fruitfully described by the statistical properties of random matrices [3]. Simple models, such as the logistic map, reveal the essence of classical chaos [4]. Comparable quantum models, such as the quantum cat map [5] and the quantum baker's map [6], while providing valuable insights, are less tractable.

The classical baker's map [4],  $T$ , is the area-preserving transformation of the unit square  $[0, 1) \times [0, 1)$  onto itself, which takes a phase space point  $(q, p)$  to  $(q', p')$  where  $(q' = 2q, p' = p/2)$  if  $0 \leq q < 1/2$  and  $(q' = 2q - 1, p' = (p + 1)/2)$  if  $1/2 \leq q < 1$ . The stretching along the horizontal  $q$  direction by a factor of 2 is compensated exactly by a compression in the vertical  $p$  direction. The repeated action of  $T$  on the square leaves the phase space mixed; this is well known to be a fully chaotic system that in a mathematically precise sense is as random as a coin toss. The area-preserving property makes this map a model of chaotic two-degree-of-freedom Hamiltonian systems, and the Lyapunov exponent is  $\ln(2)$  per iteration.

The baker's map was quantized by Balazs and Voros [6], while Saraceno [7] imposed antiperiodic boundary conditions. We consider exclusively the case  $N = 2^K$  for integer  $K$ . It has been known from early on that this case is special for the quantum baker's map [6], but this has not so far been made use of to analyze eigenstates more closely. The quantum baker's map, in the position representation, that we use in this paper is

$$B = G_K^{-1} \begin{pmatrix} G_{K-1} & 0 \\ 0 & G_{K-1} \end{pmatrix}, \quad (1)$$

where  $(G_K)_{mn} = \langle p_m | q_n \rangle = \exp[-2\pi i(m + 1/2)(n + 1/2)/N] / \sqrt{N}$ . The Hilbert space is finite dimensional, the dimensionality  $N$  being the scaled inverse Planck constant ( $N = 1/h$ ); where we have used that, the phase-space area is unity. The position and momentum states are denoted as  $|q_n\rangle$  and  $|p_m\rangle$ , where  $m, n = 0, \dots, N-1$  and the transformation function be-

tween these bases is the finite Fourier transform  $G_K$  given above. The choice of antiperiodic boundary conditions fully preserves parity symmetry, here called  $R$ , which is such that  $R|q_n\rangle = |q_{N-n-1}\rangle$ . Time-reversal symmetry is also present and implies in the context of the quantum baker's map that an overall phase can be chosen such that the momentum and position representations are complex conjugates:  $G_K \phi = \phi^*$ , if  $\phi$  is an eigenstate in the position basis.  $B$  is a unitary matrix, whose repeated application is the quantum version of the full left shift of classical chaos. There is a semiclassical trace formula, which, based on the unstable periodic orbits, approximates eigenvalues [8].

Our first step in identifying special states is to Walsh-Hadamard (WH) transform [9] eigenstates; if  $\phi$  is an eigenstate, we study  $H_K \phi$ , where  $H_K = \otimes^K H$ , a  $K$ -fold tensor product of the Hadamard matrix  $H = ((1, 1), (1, -1)) / \sqrt{2}$ . Very significant simplifications are seen in this basis for almost all states. In particular we analyze the number of principal components in the WH transform by means of the participation ratio ( $PR_H$ ), which is  $1/\sum_i |(H_K \phi)_i|^4$ . In Fig. 1 we compare this participation ratio with that calculated in the original position basis. For one remarkable class of states that is

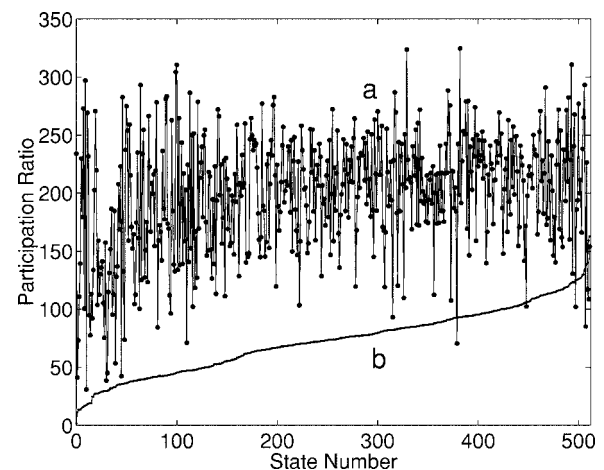


FIG. 1. The participation ratio of the eigenstates of the quantum baker's map for  $N = 512$  in the (a) position basis, and (b) Walsh-Hadamard basis. The states are arranged in increasing order of the latter number.

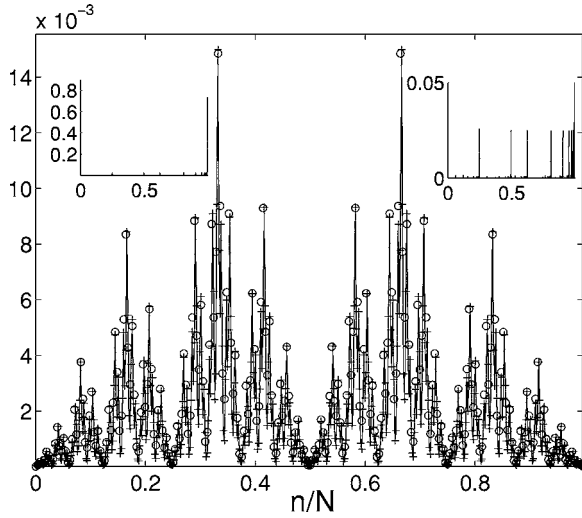


FIG. 2. The intensity  $|\langle q_n | \phi_m \rangle|^2$  of the Thue-Morse state in the position representation. Shown are the states for  $N=512$  (plus) and  $N=256$  (circle) after the latter state was appropriately scaled. Also shown is the estimate  $\phi_m^A$  for  $N=512$  case (line). The left inset is the intensity of the WH transform of the Thue-Morse state for  $N=512$ , while the right inset shows the same on a different scale.

present for all  $N$ , powers of 2,  $\text{PR}_H$  is the smallest and of the order of unity, for example when  $N=1024$ ,  $\text{PR}_H=1.96$  for this state. This class of states seems to have been identified by Balazs and Voros [6], as the eigenvalue is very close to  $-i$ ; however, the WH transform reveals their simplicity and beauty. In Fig. 2 are examples of these states, and their WH transform, where we also see their near self-similarity. We call these set of states,  $\phi_m$  the ‘‘Thue-Morse’’ states, as the principal peak in the Hadamard transform corresponds to the overlap with the final column (or row) of  $H_K$ , that (apart from the factor  $1/\sqrt{2^K}$ ) is the  $K$ th generation of the Thue-Morse sequence.

The Thue-Morse sequence is an example of a binary ‘‘automatic sequence’’ [10], whose first few terms are  $\{1, -1, -1, 1, -1, 1, 1, -1, \dots\}$ . The finite generations are constructed as follows: start with  $t_0=\{1\}$  and generate  $t_1=\{1, -1\}$  by appending  $t_0$  to  $t_0$ , where the overbar is multiplication by  $-1$ , and we continue to iterate the rule  $t_{k+1}=\{t_k, \bar{t}_k\}$ . At stage  $K$  we get  $t_K$  a string of length  $2^K$ , which we also treat as a column vector whose  $n$ th element we denote as  $t_K(n)$ . The concatenation rule above is then equivalent to the generating rules:  $t_K(2n)=t_{K-1}(n)$  and  $t_K(2n+1)=-t_{K-1}(n)$ . The Thue-Morse sequence considered as a word with two alphabets is cube free; that is, no block repeats thrice consecutively. This sequence occurs in numerous contexts [10], and is marginal between a quasiperiodic sequence and a chaotic one. The deterministic disorder of this sequence is relevant to models of quasicrystals [11] and mesoscopic disordered systems [12], and, as we show here, quantum chaos. We report that it has emerged naturally in a quantum mechanical problem, rather than being assumed.

That  $t_K$  is an approximate eigenvector of  $B$  follows on using the concatenation rule to get

$$(Bt_K)_l = \frac{\sqrt{2}}{N} C_l \sum_{m=0}^{N/2-1} t_{K-1}(m) \sum_{n=0}^{N/2-1} e^{(2\pi i/N)(n+1/2)(l-2m-1/2)},$$

where  $C_l = [1 - i(-1)^l]$ . For large  $N$  the  $n$  sum sharply peaks at  $l=2m$ , or  $2m+1$  depending on if  $l$  is even or odd. Thus  $(Bt_K)_{2m} \approx -i(2\sqrt{2}/\pi)t_{K-1}(m)$  and  $(Bt_K)_{2m+1} \approx i(2\sqrt{2}/\pi)t_{K-1}(m)$ , from which, using the generating rules of the Thue-Morse sequence, we get  $(Bt_K)_m \approx -i(2\sqrt{2}/\pi)t_K(m)$ . The eigenvalue we get has a modulus  $\approx 0.9$ . We can alternatively calculate exactly  $G_K t_K$  as a product if we use the fact that  $t_K(n)$  is  $(-1)^r$  where  $r$  is the number of times that 1 occurs in the binary representation of  $n$ . A short calculation gives

$$(G_K t_K)_m = \sqrt{2^K} (-1)^{m+1} (i)^{K+1} \prod_{j=0}^{K-1} \sin[\pi 2^{j-K} (m+1/2)],$$

a useful formula from which we can also see that  $t_K$  is an approximate eigenvector of  $B$ .

For example when  $N=2^9$ ,  $|\langle t_9 | \phi_m \rangle|^2 / N \approx 0.74$ . Taking into account symmetries helps us do much better. It is easy to see that  $Rt_K = (-1)^K t_K$ , and indeed the parity of the Thue-Morse state flips with each power of 2. We note, however, that  $G_K t_K \neq t_K$  and therefore  $t_K$  as such does not have the correct symmetry properties. To take advantage of time-reversal symmetry we construct  $\phi_0 = \gamma t_K + \gamma^* G_K^{-1} t_K$ , which satisfies  $G_K \phi_0 = \phi_0^*$ . It is straightforward to see that  $G_K^{-1} t_K$  is also an approximate eigenstate of  $B$ . We determine numerically the complex constant  $\gamma$  such that  $\phi_0$  best approximates the state  $\phi_m$ . For example if  $N=512$ ,  $\gamma$  is predominantly real and just  $\phi_0 = C(t_9 + G_9 t_9)$  is such that  $|\langle \phi_0 | \phi_m \rangle|^2 \approx 0.93$ , that is, the state  $\phi_m$  is determined to more than 93% by the Thue-Morse sequence and its Fourier transform.  $C$  is a normalization factor, and we have used that  $G_9^{-1} t_9 = G_9 t_9$ . Thus the deterministic structural disorder of the Thue-Morse sequence is seen in a quantized model of a classically deterministic and fully chaotic system.

We note that we can improve upon the simple ansatz  $\phi_0$  above, by taking into account the second rung of peaks in the Hadamard transform of  $\phi_m$ ,  $K$  easily identifiable peaks ( $N=2^K$ ), as seen for example in the right inset of Fig. 2. This second rung of peaks also results from the Fourier transform of the Thue-Morse sequence, but not exclusively. We introduce the notation  $t_k^{(r)}$  for a  $2^r$ -fold repetition of the Thue-Morse sequence of generation  $k$ ; for example, column number  $2^{K-r}-1$  of  $H_K$  is  $t_{K-r}^{(r)}$ . The improved ansatz for the Thue-Morse state is then  $\phi_m^A = \gamma_0 \phi_0 + \sum_{k=1}^K (\gamma_k + \gamma_k^* G_k^{-1}) S^{k-1} t_{K-2}^{(2)}$ , where  $S$  is the shift operator, and we again determine the complex constants  $\gamma_k$  numerically such that the ansatz is closest to the state.

The shift operator  $S$  acts on the position basis as  $S|q_n\rangle = |q_{2n}\rangle$  or  $|q_{2n-N+1}\rangle$ , depending on if  $n < N/2$  or otherwise. We notice that  $S$  is ‘‘almost’’  $B$ , only there is no momentum cutoff, as  $\langle p_m | B | q_n \rangle = \sqrt{2} \langle p_m | q_{2n} \rangle$  for  $n$  and  $m$  both  $\leq N/2-1$ . In fact,  $S$  was proposed as the quantum baker’s map by Penrose [15], however, apart from other issues, it does not respect time-reversal symmetry, in the sense that  $G_K^{-1} S^* G_K \neq S^{-1}$ . If the position state  $|q_n\rangle$  is denoted in terms

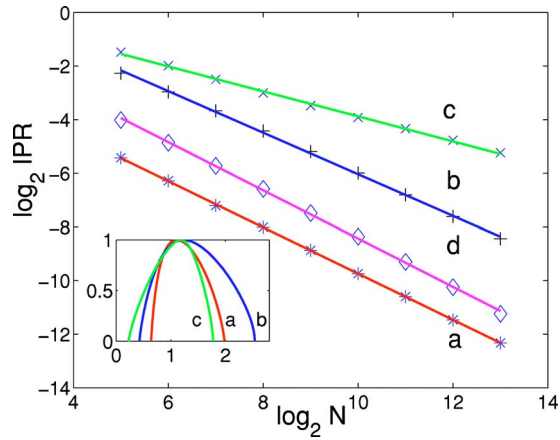


FIG. 3. (Color online) The scaling of the IPR in the position basis as a function of  $N$ . Shown as points are the numerical data, while the smooth curves are the best fit straight lines. The cases are: (a) the Thue-Morse state, (b) a period-2 scarred state, (c) a fixed-point scarred state after projecting out the uniform state, and (d) the average over all the states. The corresponding  $f(\alpha)$  spectra for the case  $N=8192$  are shown in the inset.

of the binary expansion of  $n=a_{K-1}a_{K-2}\cdots a_0$  then  $S|a_{K-1}a_{K-2}\cdots a_0\rangle=|a_{K-2}a_{K-3}\cdots a_0a_{K-1}\rangle$ , hence  $S^K=1_N$ . Such shift operators including momentum-like bits were recently proposed as quantum baker's maps; however, these also do not seem to respect time-reversal symmetry [16]. We can find  $\gamma_k$  such that  $|\langle\phi_{im}|\phi_{im}^A\rangle|^2\approx 0.998$ ; this is shown in Fig. 2. The emergence of the shift operator is unsurprising as it commutes with the Hadamard transform  $H_K$ , and is close to the quantum baker's map  $B$ . The Thue-Morse sequence  $t_K$  is an exact eigenstate of  $S$  and is hence a stand-alone state.

It is known that the support of the spectral measure of the infinite Thue-Morse sequence is a multifractal [13]; thus it comes as no surprise that  $\phi_{im}$  has multifractal properties. We can study these either by comparing Thue-Morse states at different values of  $K$  or for a fixed  $K$ , by averaging over different sized bins. We perform a standard multifractal analysis [14] and see a typical  $f(\alpha)$  singularity spectrum. One simple diagnostic is the scaling of the inverse participation ratio (IPR). If  $\phi_n$  denotes the position representation of the state  $\phi$ , the IPR that is  $\sum_{n=0}^{N-1} |\phi_n|^4$  scales as  $N^{-D_2}$ . When  $D_2$ , the correlation dimension, is such that  $0 < D_2 < 1$ , the function is a multifractal, between localized states ( $D_2=0$ ) and random states ( $D_2=1$ ). This IPR and multifractal analysis is carried out in the physically relevant position basis. Either of the two procedures gives, for the Thue-Morse state, the dimension  $D_2\approx 0.86$ , indicating its multifractal character. This scaling along with the full  $f(\alpha)$  spectrum is shown in Fig. 3.

The Thue-Morse state is by far not the only one influenced by the Thue-Morse sequence. We now construct a family of strongly scarred states consisting of  $K$  members. The  $\text{PR}_H$  is low for these states also, for example when  $N=512$   $\text{PR}_H\sim 15$ . We identify this as a "family" based on the similarity of their  $\text{PR}_H$  and the shared position of the  $K$  principal peaks in their WH transform. For up to  $N=2^{13}$  we have verified that this family exists and has  $K$  prominent peaks, at

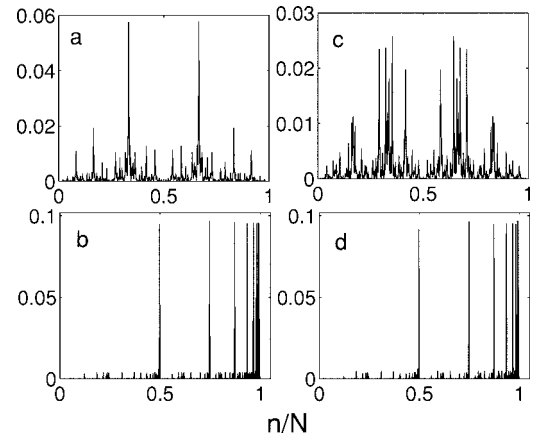


FIG. 4. Two members of a family scarred by the period-2 orbit for  $N=512$ . Shown are the intensities (in position basis) of the states in (a) and (c), while the corresponding WH transforms are shown in (b) and (d).

$t_{K-1}^{(1)}$  and all its  $K-1$  shifts,  $S^k t_{K-1}^{(1)}$ . Among this family, members are strongly scarred by period-2, period-4, and related homoclinic orbits. Two examples of the members of this family along with their WH transforms are shown in Fig. 4. Taking time-reversal symmetry into account we may then write an approximate expression for this family of states based on  $K$  vectors, similar to the one above for the Thue-Morse state. For example for  $N=512$  this procedure enables us to reproduce the state strongly scarred by the period-2 orbit up to more than 95% and most of the family to similar accuracy. The existence of such families may be indicative of systematics of periodic orbit scarring.

This strongly scarred state and its family members also have multifractal properties, and indeed  $D_2\approx 0.8$  for the period-2 scarred state (Fig. 3). We have identified other families, but we now turn to the state that is strongly scarred by the fixed point (0,0) and whose WH transform is strongly peaked, indeed corresponding to  $t_0^{(K)}/\sqrt{2^K}$ , that is simply the uniform state. This also forms a series, for different  $N$ , whose eigenangles are close to zero. Since the Fourier transform of

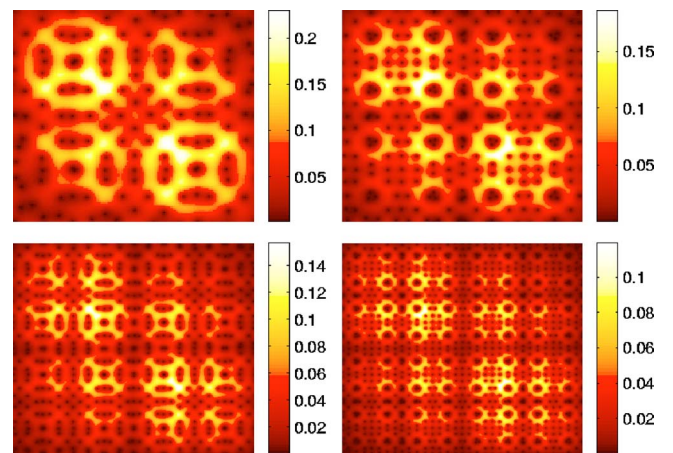


FIG. 5. (Color online) The density plots of  $|\langle qp|\psi\rangle|$  on the unit phase-space square for the Thue-Morse state in the cases  $N=128$ , 256, 512, and 1024 (left to right, top to bottom).

the uniform state given above tends to a constant (independent of  $N$ ) at the origin (and at 1), we expect the scarred state to be dominated by this “Bragg peak.” In order to see any multifractal character even in this state, we project  $t_0^{(K)}$  out of its WH transform and analyze the resultant state (after renormalizing) in the position basis. This shows that the “grass” even in this strongly scarred state is a multifractal with a value of  $D_2 \approx 0.45$ , as shown in Fig. 3, where the  $f(\alpha)$  spectrum for the fixed point and the period-2 scarred states are also shown conforming to those expected of multifractals. For a gross measure of the multifractality of the entire spectrum, we averaged the IPR (in the position basis) of all the states and found a scaling with  $D_2 \approx 0.9$  that is shown in Fig. 3.

Classical structures in quantum states are clearly seen in their phase-space or coherent state representations [7], which is shown in Fig. 5 for the Thue-Morse states we have discussed above. Note the self-similarity of the four states shown here; the two different types of intricate structures arise from the alternating parity of these states. While dominated by the period-2 orbit and its associated structures, we leave the details for a later work.

We have merely skimmed the surface of the states in this paper, highlighting the features found. The classical baker’s map straightens out the intricate homoclinic tangle of unstable and stable manifolds to lie along the  $q$  and  $p$  directions, which are also the basis in which we are viewing the quantum states. The multifractality and the simplicity of the states may originate in this, while in other models the complexity of the tangle may give rise to a “mixing” that makes them look random. That the dimensionality is a power of 2 is also a critical requirement for the observations in this paper. Qubit implementation of the quantum baker’s map, such as the experimental work with NMR bits [17] are naturally of this kind. However, self-similarity has been noticed indirectly earlier in the quantum baker’s map in the correlations between the eigenstates and level velocities [18], even for  $N$  that are not powers of 2.

N.M. was supported by financial assistance from the Council for Scientific and Industrial Research, India. We thank H. R. Naren for involvement in the early stages of this work.

- 
- [1] M. V. Berry, Proc. R. Soc. London, Ser. A **413**, 183 (1987).
  - [2] E. J. Heller, Phys. Rev. Lett. **53**, 1515 (1984); in *Les Houches LIII, Chaos and Quantum Physics*, edited by M.-J. Giannoni, A. Voros, and J. Zinn-Justin (North-Holland, Amsterdam, 1991).
  - [3] F. Haake, *Quantum Signatures of Chaos* (Springer, Berlin, 1991).
  - [4] A. J. Lichtenberg and M. A. Leiberman, *Regular and Chaotic Dynamics* (Springer, New York, 1992).
  - [5] J. H. Hannay and M. V. Berry, Physica D **1**, 267 (1980); J. P. Keating, Nonlinearity **4**, 309 (1991).
  - [6] N. L. Balazs and A. Voros, Ann. Phys. (N.Y.) **190**, 1 (1989).
  - [7] M. Saraceno, Ann. Phys. (N.Y.) **199**, 37 (1990).
  - [8] A. M. Ozorio de Almeida and M. Saraceno, Ann. Phys. (N.Y.) **210**, 1 (1991); M. Saraceno and A. Voros, Physica D **79**, 206 (1994).
  - [9] M. R. Schroeder, *Number Theory in Science and Communication* (Springer, Berlin, 1986).
  - [10] J.-P. Allouche and J. Shallit, in *Sequences and Their Applications*, Proceedings of the 1998 SETA Conference, edited by C. Ding, T. Helleseth, and H. Niederreiter (Springer, Berlin, 1999); *Automatic Sequences: Theory, Applications and Generalizations* (Cambridge University Press, Cambridge, 2003).
  - [11] A. Bovier and J.-M. Ghez, J. Phys. A **28**, 2313 (1995).
  - [12] M. Janssen, Phys. Rep. **295**, 1 (1998); A. D. Mirlin, *ibid.* **326**, 259 (2000).
  - [13] C. Godreche and J. M. Luck, J. Phys. A **23**, 3769 (1990); M. A. Zaks, A. S. Pikovsky, and J. Kurths, *ibid.* **32**, 1523 (1999).
  - [14] T. C. Halsey, M. H. Jensen, L. P. Kadanoff, I. Procaccia, and B. I. Shraiman, Phys. Rev. A **33**, 1141 (1986).
  - [15] O. Penrose, *Foundations of Statistical Mechanics* (Pergamon Press, New York, 1970).
  - [16] R. Schack and C. M. Caves, Appl. Algebra Eng. Commun. Comput. **10**, 305 (2000).
  - [17] Y. S. Weinstein, S. Lloyd, J. V. Emerson, and D. G. Cory, Phys. Rev. Lett. **89**, 157902 (2002).
  - [18] A. Lakshminarayan, N. R. Cerruti, and S. Tomsovic, Phys. Rev. E **63**, 016209 (2000).